RSC Advances

Surface modification of polyamide composite membranes by corona air plasma for gas separation applications

Journal:	*RSC Advances*
Manuscript ID:	RA-ART-12-2014-015547.R1
Article Type:	Paper
Date Submitted by the Author:	25-Jan-2015

Complete List of Authors:	Zarshenas, Kiyoumars; Amirkabir University of Technology (Tehran Polytechnic), Department of Chemical Engineering Raisi , Ahmadreza ; Amirkabir University of Technology (Tehran Polytechnic), Department of Chemical Engineering Aroujalian, A.; Amirkabir University of Technology (Tehran Polytechnic), Department of Chemical Engineering

Journal Name

RSCPublishing

ARTICLE

Surface modification of polyamide composite membranes by corona air plasma for gas separation applications

Cite this: DOI: 10.1039/xoxxoooooox

Received ooth January 2014,
Accepted ooth January 2014

DOI: 10.1039/xoxxoooooox

www.rsc.org/

Kiyoumars Zarshenas,[a] Ahmadreza Raisi [a,b,*] Abdolreza Aroujalian [a,b]

In this study, dual-layer polyamide 6/polyethersulfone (PA6/PES) composite membranes were prepared via the phase inversion technique and corona air plasma was employed to modify the membrane surface in order to improve the gas separation performance. The effect of corona treatment parameters like exposure time and input power on the membrane surface properties, morphology and separation performance was investigated. The gas separation performance of the membranes before and after the corona treatment was evaluated by permeation measurement for CO_2, O_2 and N_2 gases. The FTIR-ATR, SEM, AFM and contact angle analysis were used to characterize the untreated and corona treated membranes. The FTIR-ATR and contact angle results indicated that the corona treatment introduced polar groups on the membrane surface and led to significant enhancement in the membrane polarity, hydrophilicity and wettability. The gas permeation results revealed that the permeability and selectivity of the modified membranes strongly changed due to surface ablation and formation of polar groups depending on the corona treatment conditions. An increase in corona treatment time and input power resulted in higher gas permeability, however corona modification at high power and longer exposure time led to a membrane with low gas selectivity.

Introduction

The membrane gas separation technology due to a number advantages in terms of low energy requirements, modular design, low capital investment, low maintenance cost, low labor intensity, environmental safety as well as easy to operate and compact equipments has been extensively investigated for various gas separation applications including air separation, hydrogen recovery and purification, flue gas separation and natural gas processing.[1-3] Both inorganic and polymeric materials have been employed to prepare membranes for the gas separation process. Various rubbery and glassy polymers like polydimethylsiloxane (PDMS), polyacetylene, poly(1-trimethylsilyl-1-propyne) (PTMSP), polyimide (PI), polyamide (PA), polyarylate, polycarbonate (PC), polyethersulfone (PES), polysulfone (PSf), polyolefins, cellulose acetate (CA) and polyphenylene oxide (PEO) have been employed for the gas separations.[4, 5] Among these polymers, polyimides have been extensively used to fabricate membrane for the gas separation applications because of high gas selectivity, excellent thermal and chemical stability, mechanical strength and good film forming properties. Polyamides are semi-crystalline polymers which have properties similar to polyimides.[6] Despite the outstanding chemical and physical properties of polyamides, this polymer was not explored much as membrane material for use in the gas separation.

Generally, despite the excellent processability, the polymeric membranes often have low separation performance. In order to improve the separation performance and properties of the polymeric membranes for the gas separation applications, various techniques such as blending, incorporation of inorganic fillers, surface modification and copolymerization have been applied. Among these methods, the surface modification method has the advantages of improving the surface characteristics including wettability and polarity without significant changes on the bulk properties of the membrane.[7] The surface modification techniques involve coating, graft

[a] Department of Chemical Engineering, Amirkabir University of Technology (Tehran Polytechnic), Hafez Ave., P.O. Box 15875-4413, Tehran, Iran.

[b] Food Process Engineering and Biotechnology Research Center, Amirkabir University of Technology (Tehran Polytechnic), Hafez Ave., P.O. Box 15875-4413, Tehran, Iran.

[*] Author for correspondence: Phone: (9821) 64543125, Fax: (9821) 66405847, E-mail: raisia@aut.ac.ir

polymerization, covalent attachment of functional monomers and cold plasma treatment.[8] Cold plasma techniques like glow discharge,[9, 10] radio frequency (RF)[11, 12] and corona discharge[13, 14] have been employed to modify the membrane surface to improve the hydrophilicity, wettability, fouling resistance and separation performance of the membrane.

Plasma techniques are very effective in polarity modification accompanied by extensive etching on the surface.[15] Generally, the cold plasma has been used as a pretreatment in the graft polymerization for surface modification of various membranes. For instance, Weibel et al.[16] employed RF plasma containing oxygen, nitrogen or acrylic acid to modify the surface of polyurethane membranes for use in the pervaporation process. Zhu et al.[17] employed the corona discharge plasma for the graft polymerization of acrylic acid onto polyethersulfone membranes to increase the fouling resistance for protein solutions. Guo et al.[18] also used the corona-induced graft polymerization for coating acrylic acid onto the high-density polyethylene microfiltration membrane to increase the hydrophilicity of the membrane. Furthermore, some researchers applied the cold plasma methods to directly modify different polymeric membranes for use in the membrane processes such as microfiltration, ultrafiltration and membrane distillation. For example, oxygen, H_2O and NH_3 plasma techniques were used by Steen et al.[11], Kim et al.[19] and Bryjak et al.[20], respectively, for modification of the polysulfone membranes to minimize the fouling phenomena in the ultrafiltration process. Also, Sadeghi et al.[14] applied the corona air plasma to modify the surface of the PES ultrafiltration membrane to enhance the surface hydrophilicity and permeation properties of the membrane. Moghimifar et al.[21] used the corona discharge treatment to alter the surface of the PES membrane for coating TiO_2 nanoparticles on the membrane surface. In addition, various cold plasma techniques were employed to alter the polymeric membranes like polyimide[7] ,polyethylene[22] , polypropylene[23] , poly(phenylenoxide)[24] , polyamide 6[25] and PSf[26, 27] in order to improve their permeation performance for use in the gas separation process. A search in the literature reveals that the use of corona air plasma for the modification of the gas separation membranes has not been previously reported.

In this work, dual-layer polyamide 6/polyethersulfone composite membranes were fabricated by the phase inversion technique and modified by corona air plasma to improve the separation performance for use in the gas separation process. The effect of the corona treatment parameters including exposure time and discharge power on the membrane surface properties and separation performance was studied. Fourier transform infrared-attenuated total reflection (FTIR-ATR) spectroscopy, scanning electron microscopy (SEM), atomic force microscopy (AFM) and contact angle analysis were used to characterize the surface properties of the modification membranes.

Experimental

Materials

The commercial PES with molecular weight of 58000 g/mol (ultrason E 6020P) and polyamide 6 (PA6) (Akulon F136-C1) purchased from BASF (Ludwigshafen, Germany) and DSM (Heerlen, Netherlands) were utilized as membrane material, respectively. Formic acid and N,N-dimethyl-formamide (DMF) as organic solvents received from Merck Co. Ltd. (Darmstadt, Germany) were used for membrane preparation. Moreover, O_2, N_2 and CO_2 gases with purity of 99.99% were utilized as feed gas in this work.

Membrane preparation

The porous PES membrane, used as a support layer for preparation of PA6/PES composite membranes were prepared by the non-solvent induced phase-inversion method. In this procedure, 16 %wt. PES was dissolved into the DMF solvent and then underwent vigorous stirring until a clear homogeneous solution was obtained. The PES solution was de-aerated by a vacuum process for 2 h and then cast on a glass plate with a casting knife. The glass plate was immediately immersed into a bath containing de-ionized water as non-solvent at room temperature. After coagulation, the formed PES membrane was separated from the glass plate. The obtained membranes were stored in a soaking bath containing de-ionized water for 24 h for complete removal of the residual solvent. Finally, the PES membranes were dried for 24 h at room temperature.

The active dense layer of the composite membrane was prepared by the solvent evaporation induced phase-inversion method. For this purpose, 15 %wt. of PA6 was dissolved in formic acid and then the prepared solution was stirred vigorously at room temperature over night to obtain a clear homogenous solution. Afterwards, the polymer solution was de-aerated by a vacuum process for 2 h. Afterwards, the bubble-free PA6 solution was cast on the porous PES support membrane which was placed on a glass plate with a casting knife. The dual-layer PA6/PES composite membrane was formed by solvent evaporation in an oven at 35 °C for 24 h. The thickness of the obtained dual-layer membranes was found to be about 100±5 μm.

Membrane modification

To modify the surface of the dual-layer PA6/PES membranes, the membrane was treated by the corona air plasma. The corona treatment of the membranes was carried out in the air at atmospheric pressure using a commercial device (Naaj Corona, Naaj Plastic, Tehran, Iran). The membrane samples with a uniform size of 5 cm × 5 cm were placed on the backing roller covered with the silicon coating and rotating at a given speed. The distance between the aluminum electrode and the backing roller was adjusted to a specific value. Corona plasma was generated within the air gap between the electrode and backing roller. The membrane samples were treated when they came into contact with the produced corona. To investigate the effect of time and power of corona treatment on the membrane modification, the corona input powers were varied within 240-

600 W and the time period of 2-8 min. The prepared membranes are named as presented in Table 1.

Table 1: The corona treatment conditions of the membranes.

Membrane sample	Corona input power (w)	Corona time (min)
M1	-	-
M2	240	4
M3	320	4
M4	400	2
M5	400	4
M6	400	6
M7	400	8
M8	500	4
M9	600	4

Gas permeation measurement

A pre-calibration cross flow flat sheet permeation cell with constant volume and variable pressure was employed for the permeation measurements. Pure gas permeation was tested in the sequence of O_2, N_2 and CO_2. The permeation experiments were conducted at constant feed temperature and pressure of 25°C and 3 bar, respectively. The pressure of the permeate was recorded at each 0.3 seconds and the rate of pressure enhancement (dp/dt) was imported to Eq. (1) for the permeation measurements. The gas permeability of the prepared membranes was determined using the following equation:

$$P = \frac{273.15 \times 10^{10}\, V\, l}{760\, A\, T\, \left(\frac{76\, p_0}{14.7}\right)} \left(\frac{dp}{dt}\right) \quad (1)$$

where P is the permeation coefficient of gas (Barrer), V is downstream volume (cm^3), A is the effective area of membrane (cm^2), T is temperature (K), po is feed pressure (psia) and l is membrane thickness (μm).

Also, the ideal selectivity of the membrane (αA/B) was calculated from the pure gas permeation experiments as follows:

$$\mathrm{J} = \frac{\mathrm{W}}{\mathrm{A.t}} \quad (2)$$

Membrane characterization

FTIR-ATR spectroscopy was used to characterize the functional groups on the membrane surface and detect the chemical changes after the corona treatment. The FTIR-ATR instrument used consisted of a Nicolet Nexus 670 spectrometer (Nicolet Instrument Co., Madison, WI, USA) with 4 cm^{-1} resolution over a wave number range of 4000–600 cm^{-1}. To observe the difference between treated and untreated membranes, for each test a 1 cm × 4 cm sample without further treatment as used and the corona treated membranes were tested right after being exposed to the corona. The morphology of the membranes was analyzed by SEM images from the top surface and cross section of the membranes with a SEM device (KYKY-EM3200 SEM, China) at an accelerated voltage of 20 KV. To observe the image of the membrane cross section, hydrate membrane samples were fractured by immersing them into liquid nitrogen. Then all virgin and treated membranes were stuck on a sample holder and the samples were coated with a thin layer of gold layer by a sputtering system before analysis.

membranes surface at room temperature with de-ionized water. The CA of four different locations on the membrane surface was measured and the average values were reported as CA for a membrane sample.

The AFM analysis was used to measure the changes of the membrane surface roughness before and after the corona treatment. The AFM tests were performed using a microscope (NanoEducator, NTMDT Co., Zelenograd, Russia) with a spatial resolution of approximately 2nm in z direction. The instrument was calibrated by standard samples (TGG1 and TGX1, NT-MDT Co., Zelenograd, Russia). The membrane samples were fixed on a holder double-sided tape and 5 μm × 5 μm areas were scanned by semi-contact mode in the air. Three different locations were tested and the average values of roughness were reported. The roughness was expressed as RMS (root mean square) and RA (average roughness) values.

Results and discussion

FTIR-ATR spectroscopy

A particular increase in the membrane surface polarity after modification by the corona treatment can be related to changes in the functional groups on the membrane surface. The FTIR-ATR spectrum of the untreated PA6/PES composite membrane is shown in Fig. 1. In this spectrum, the amide bands of the PA6 layer appear at 1631 and 1533 cm^{-1} and N-H, CH_2 (asymmetric stretching) and CH_2 (symmetric stretching) groups reveal at wave number of 3288, 2921 and 2850 cm^{-1}, respectively. Also, the peaks between 1200 and 900 cm^{-1} can be ascribed to the skeletal aliphatic C-C and aliphatic C-H rocking of the polyamide.

To recognize the changes in the functional groups of the membrane surface after the corona treatment, the FTIR-ATR spectra of the untreated membrane and corona treated PA6/PES sample at the corona power of 400 W and treatment time of 4 min are indicated in Fig. 2. Also, the ratio of absorbance intensity of different functional groups with respect to that of the C-C group in these spectra is given in Table 2.

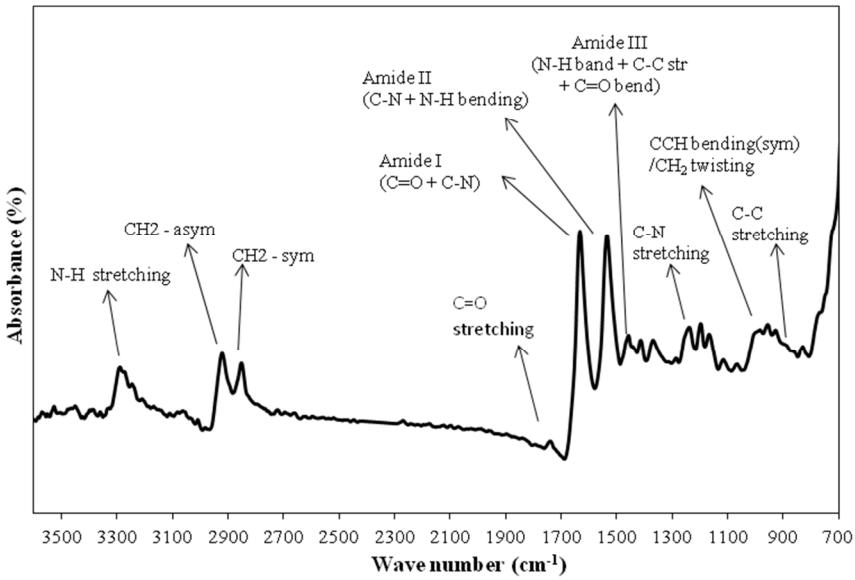

Fig. 1: The FTIR-ATR spectrum of the untreated PA6/PES membrane.

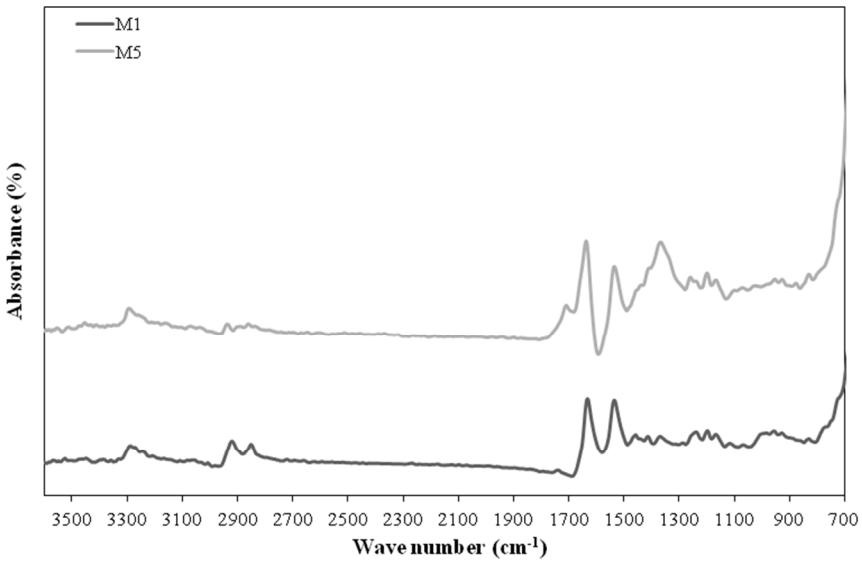

Fig. 2: The FTIR-ATR spectra of the untreated and corona treated membrane (M5 membrane sample).

It can obviously observed from Table 2 that the relative ratio of functional groups like C-N, C=O and amide bands to the C-C group increases by the corona treatment of the polyamide layer of the composite membrane. In the corona air plasma, the corona ionizes the oxygen and nitrogen molecules in the atmosphere and produces the ionized species and radicals. These charged compounds attack the membrane surface leading to C-C and C-H bond scission and formation of polar groups like C-O, C=O and C-N. Table 2 also shows that the value of normalized peak intensity for amide groups enhances for the corona treated membrane. This indicates the formation of additional amide groups due to the presence of oxygen in the plasma zone. Similar results were reported for the O_2 plasma treatment of nylon fabrics.[28]

Besides, the influence of the corona treatment conditions on the surface changes of the PA6/PES composite membranes was investigated. The effect of corona input power at constant treatment time on the surface modification of the membranes is indicated in Fig. 3. The FTIR-ATR spectra in this figure reveal that the absorbance intensity of C=O, C-N, amide I, amide II and amide III groups at the corona power of 400 W is greater than other corona powers. As discussed by Sadeghi et al.[14] and Moghimifar et al.[21] , the effect of corona treatment conditions on the surface modification can be related to the building effect and damaging effect during corona treatment. These possible

phenomena may counteract one another or overtake the other; therefore depending on the power and time of the corona treatment, different effects can be seen at different stages. When the corona input power increases from 240 to 400 W, the building effect is dominated, i.e. the corona treatment at these input powers leads to formation of more functional groups on the membrane surface due to creation of more radical sites through the bond opening and reaction with the ionized species in the corona gas. However, at high corona input power (600 W), the formation of active sites on the membrane surface slows down and the damaging effect eventually dominates. At this stage, the damaging effect of the corona treatment leads to a decrease in the absorbance intensity of the functional groups such as amides as well as C=O and C-N groups.

Table 2: The ratio of absorbance intensity of different functional groups to C-C group in the FTIR-ATR spectra of the M1 and M5 membranes.

Ratio of functional group	M1	M5
C-N stretching/C-C stretching	0.989	1.117
Amide III/C-C stretching	0.925	1.525
Amide II/C-C stretching	1.193	1.242
Amide I/C-C stretching	1.494	1.542
C=O stretching/C-C stretching	0.387	0.783
N-H stretching/C-C stretching	0.774	0.742

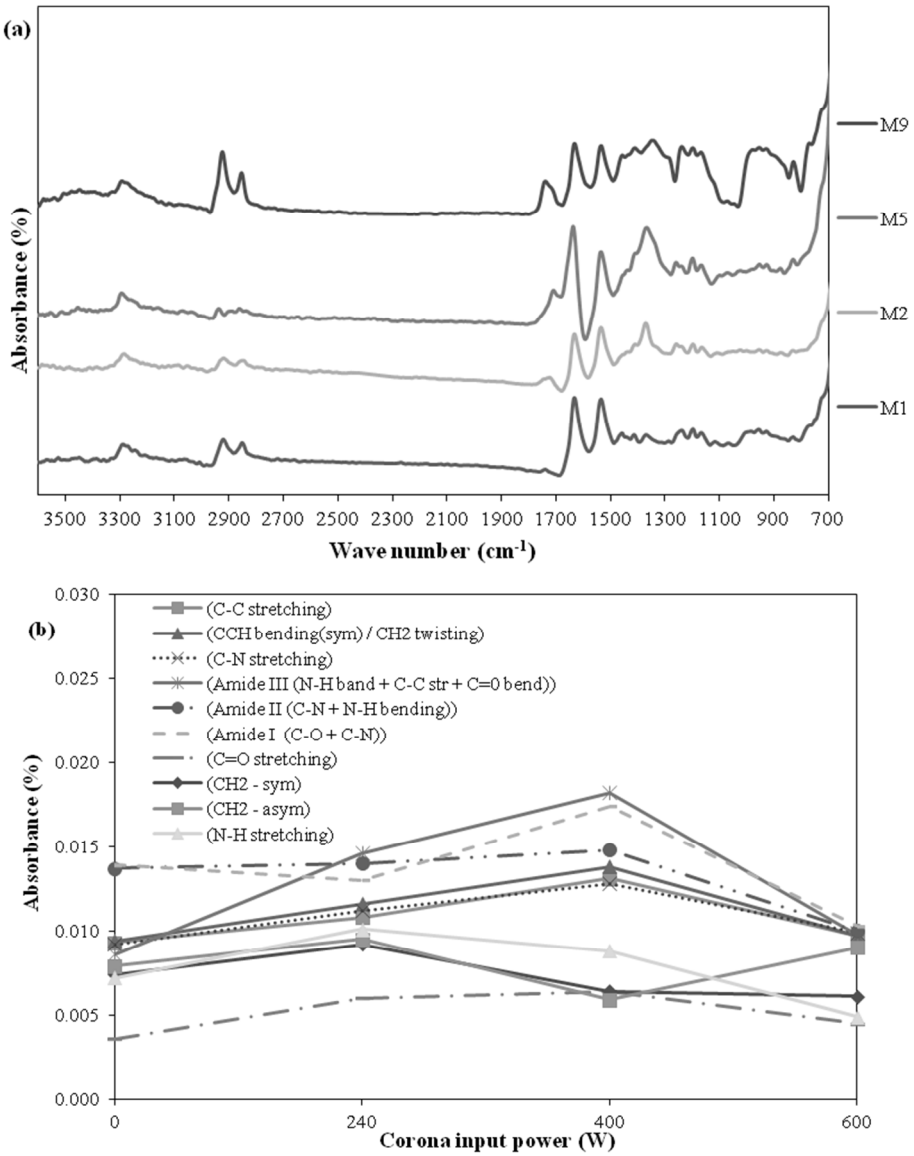

Fig. 3: The effect of corona input power on the surface modification of PA6/PES membrane for treatment time of 4min: (a) the FTIR-ATR spectra and (b) the peaks absorbance.

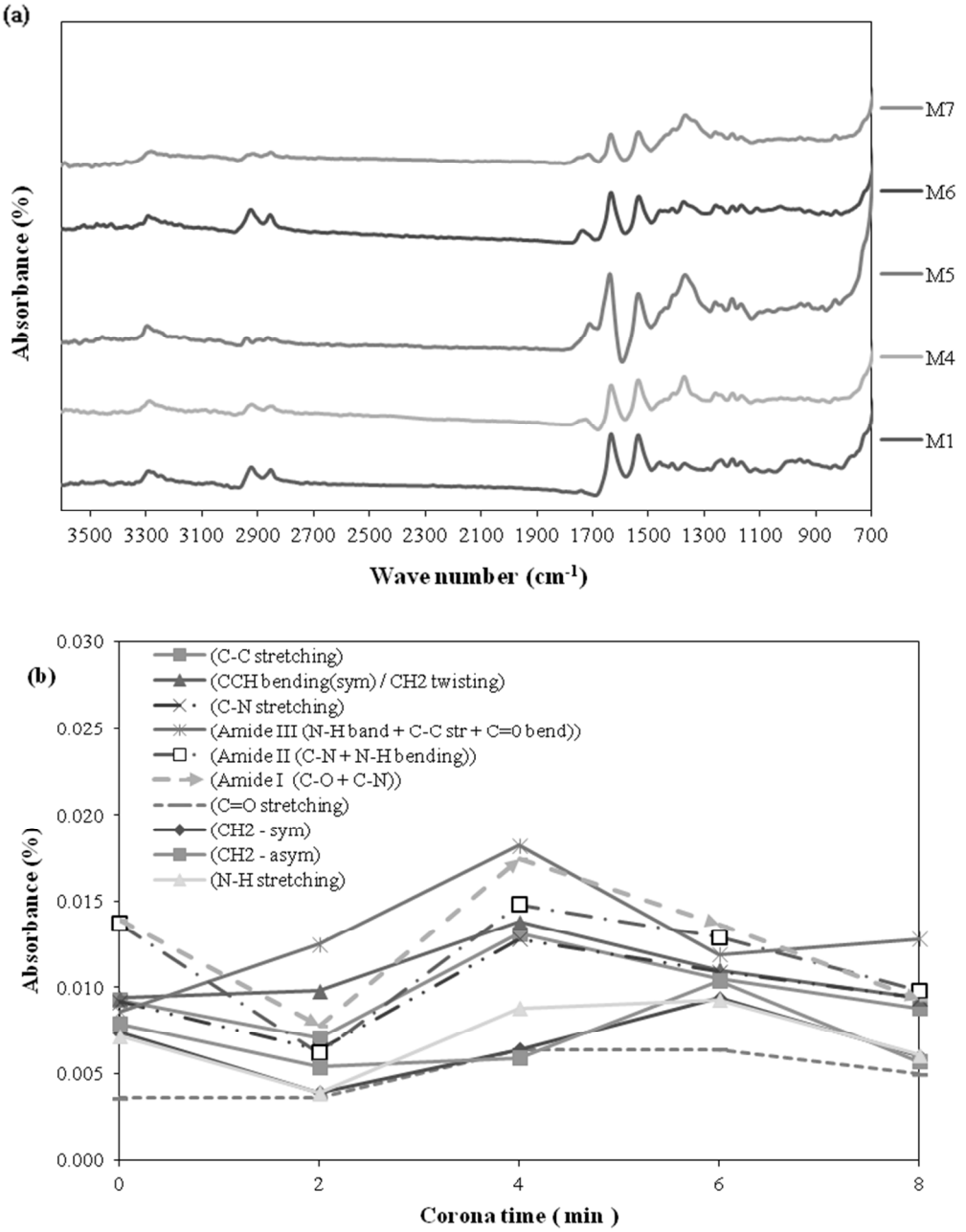

Fig. 4: The effect of corona treatment time at constant power 400 W on the surface modification of PA6/PES membrane: (a) the ATR-FTIR spectra and (b) the peaks absorbance.

The influence of the corona treatment time on the absorbance intensity of peaks and the functional group composition is shown in Fig. 4. By comparing the FTIR-ATR spectra of the untreated membrane and corona treated samples, it can be seen that at short exposure to corona (2 min), initial degradation of all bonds occurs, and during this stage, new bonds are not yet formed so a little lowering in the absorbance intensity of all bonds is discernible. At exposure time of 4 min, the absorbance of amide I, amide II, amide III, C=O and C-N groups as polar functional groups arrive at their maximum intensity and at corona treatment times higher than 4min, a continues decline in all bonds is observed. This trend can be attributed to the damaging effect of the corona air plasma. [12, 20]

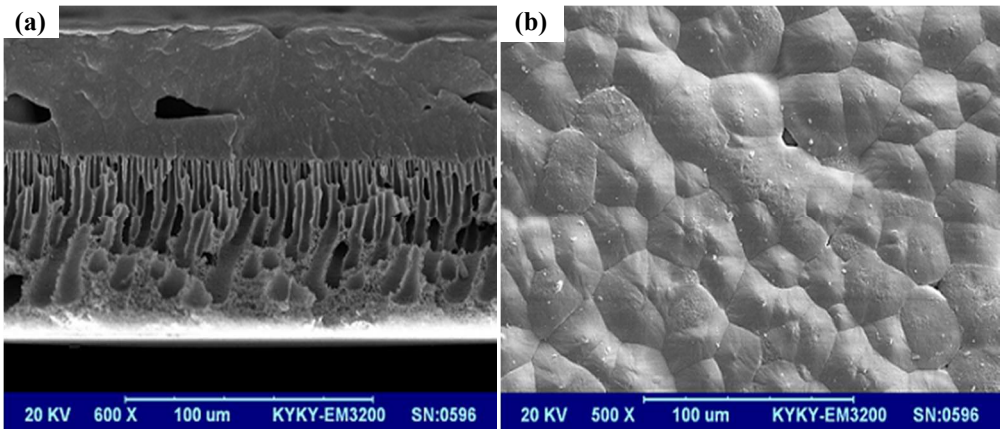

Fig. 5 The SEM images from cross section (a) and top surface (b) of the untreated PA6/PES composite membrane.

SEM analysis

The SEM analysis was used to determine changes in the membrane morphology due to the corona air plasma modification. The SEM images from the cross section and top surface of the PA6/PES membrane before the corona treatment are presented in Fig. 5. As shown in this figure, the dual-layer PA6/PES composite membrane prepared by the phase-inversion method has a dense top layer, PA6, on a support, PES layer, with a finger like structure. It can be observed from Fig. 5a that the top surface of the membrane is a nonporous dense layer containing polygonal grains.

The SEM images from the top surface of the untreated membrane and the modified membranes at different corona treatment times and input powers are shown in Fig. 6. The etching effect of the corona treatment on the membrane surface can clearly be observed in these SEM micrographs. It can be seen that all modified membranes have a different top surface in comparison to the untreated membrane sample and an enhancement in the corona exposure time and input power results in a progressive rugged surface. In other words, the physical effect of the corona modification becomes more pronounced with an increase in the corona treatment time or input power. As the corona power increases, more ionized molecules are generated in the plasma zone and consequently ion bombardment of the membrane surface will be more severe, and therefore the membrane surface is etched more harshly. The same reason can be expressed for the influence of the corona treatment time on the morphology of the membrane surface.

AFM analysis

The AFM analysis was also applied to analyze the effect of corona power and exposure time on the surface roughness of the PA6/PES membranes. Fig. 7 indicates three dimensional topographic AFM images of different membranes. Also, the values of average roughness (RA) and root mean square of the Z data (RMS) of different membranes as a function of corona treatment time and input power are presented in Fig. 8. The influence of the corona exposure time on the surface roughness at applied corona power of 400 W is indicated in Fig. 8a. As shown in this figure, both RA and RMS values have a minimum and maximum point at exposure time of 2 and 4 min, respectively. At a shorter time (2 min), the ablation and etching effects of the corona treatment cause the surface roughness to slightly increase and result in a rougher surface. By increasing the corona treatment time, the chemical effect of the corona treatment changes the composition of functional groups on the membrane surface and introduces various functional groups which can be observed obviously from the FTIR-ATR spectra, and this can change surface morphology. Moreover, deposition of the etching materials on the membrane surface just after etching may make the surface softer as can be seen clearly from the SEM images (Fig. 6c). Thus, the Ra and RMS values decrease at treatment time of 4 min. A further increase in the corona treatment time results in further etching effect of the corona modification and consequently the surface roughness enhances. On the other hand, ion bombardment separates the deposited pieces and makes some cracks on the membrane surface as could be seen from SEM images (Fig. 6f). These results are consistent with the study of Sadeghi et al.[14] and Moghimifar et al.[21] which used the corona air plasma for modification of the PES membrane.

Besides, the same trend was seen as the corona applied power varied from 240 to 600 W at a constant exposure time of 4 min on the surface roughness as revealed in Fig. 8b. It can be seen that the surface roughness slightly increases at the input power of 240 W and decreases significantly by increasing the power to 400 W. Then the membrane surface roughness enhances by a further increase in the corona applied power.

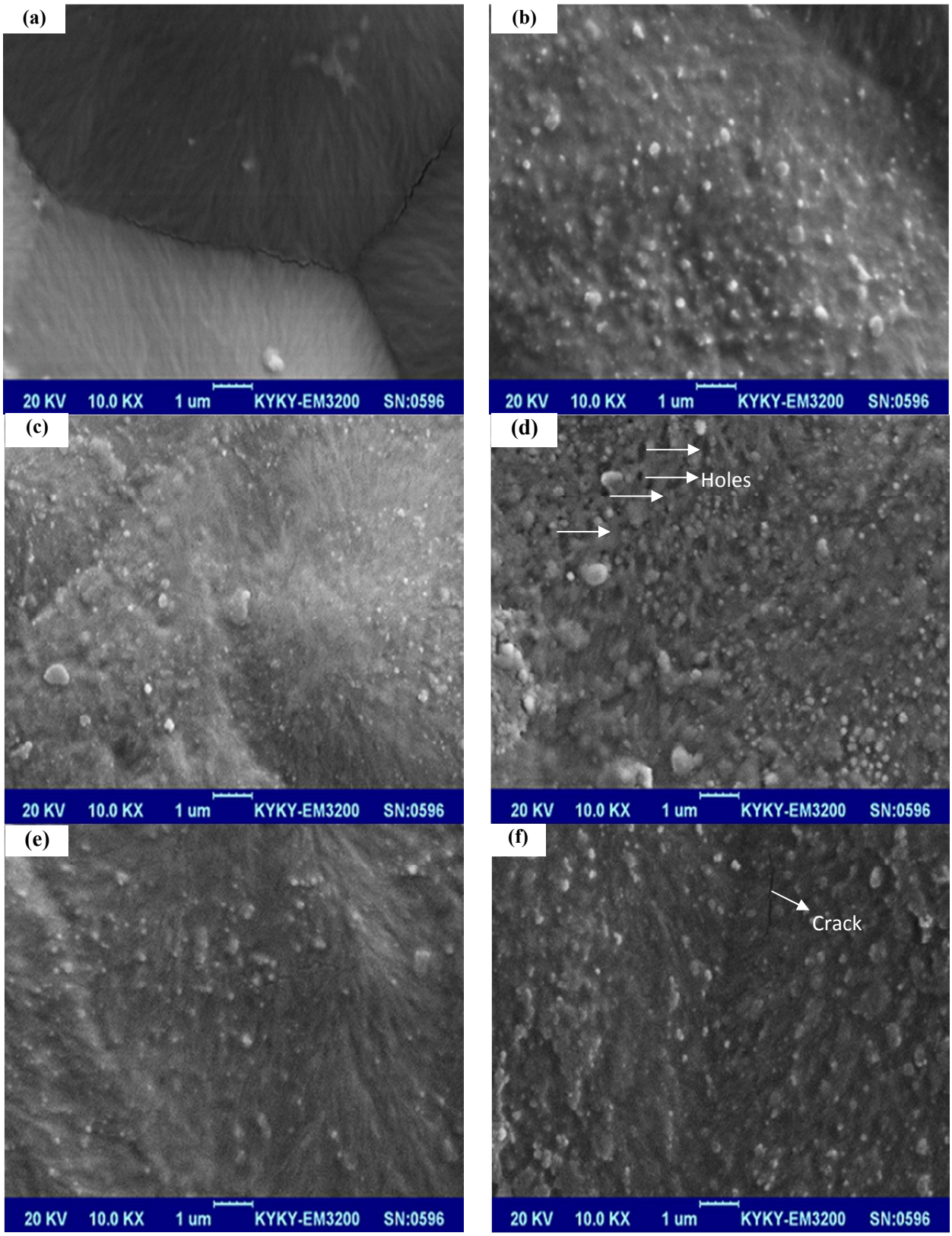

Fig. 6: The SEM images from the top surface of the PA6/PES composite membranes: a) M1, b) M2, c) M5, d) M9, e) M4 and f) M6.

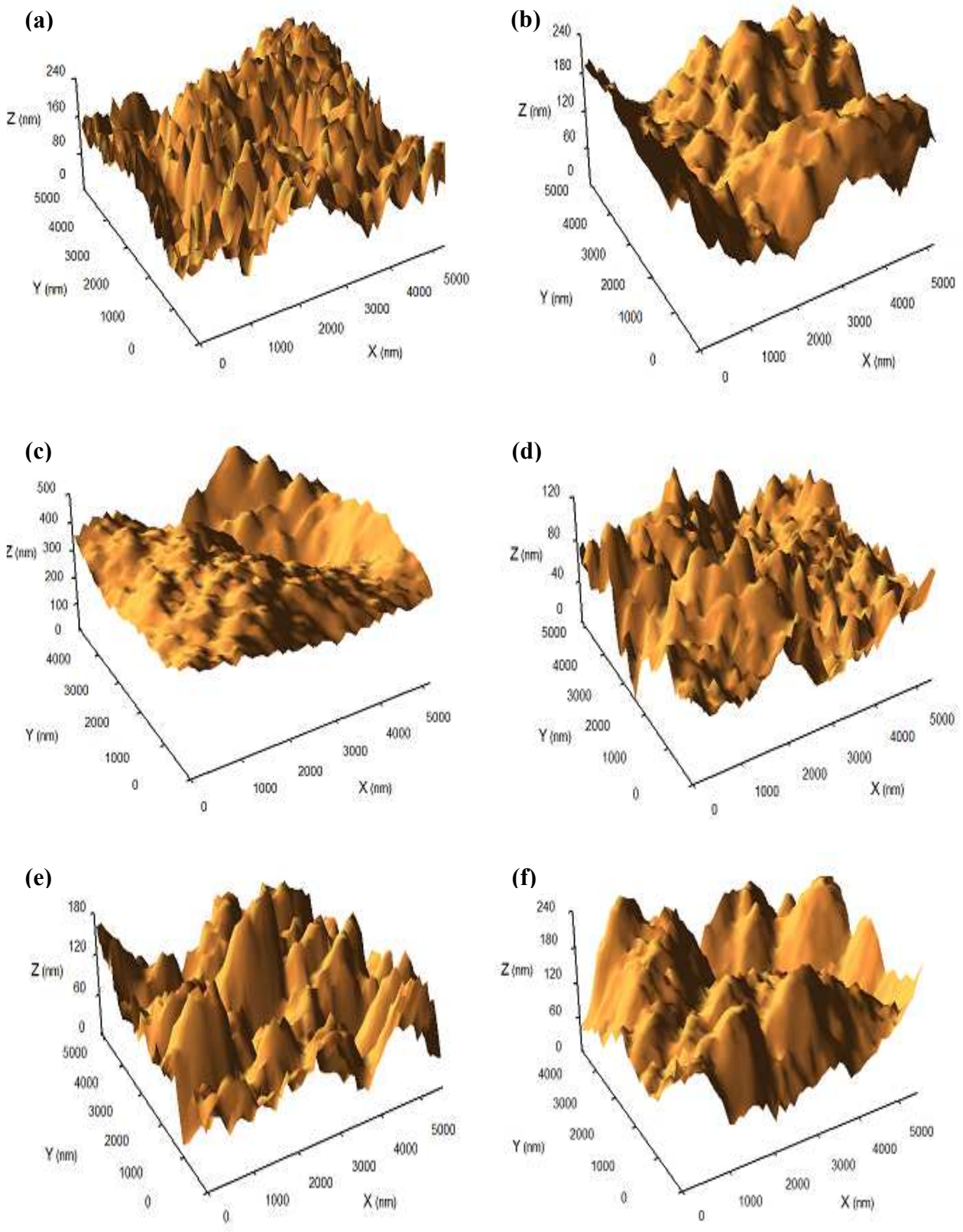

Fig. 7: The AFM images of the PA6/PES composite membranes: a) M1, b) M2, c) M4, d) M5, e) M6 and f) M9.

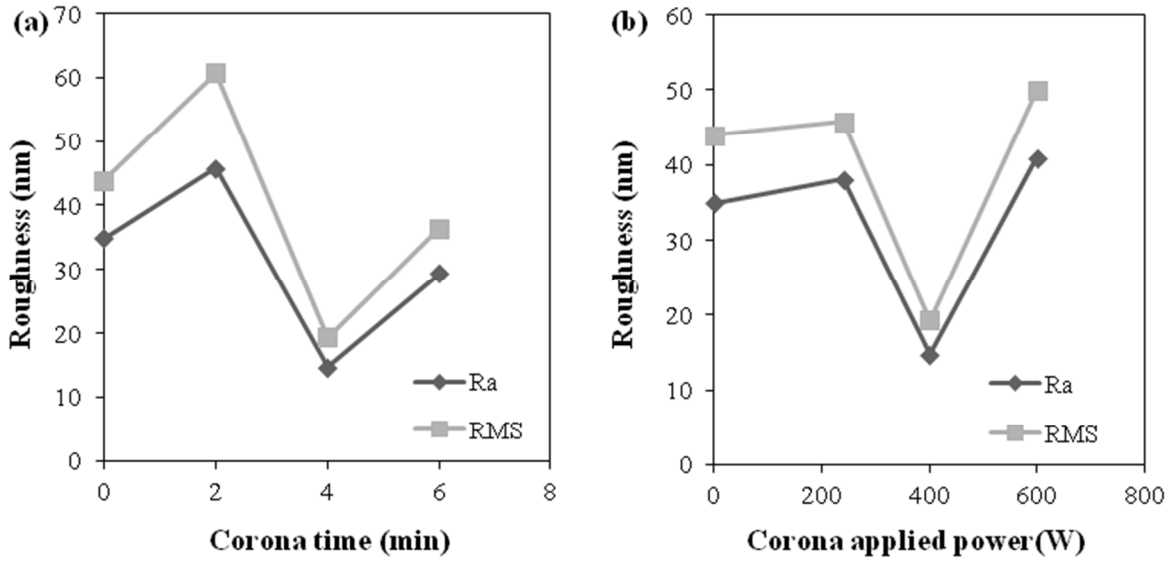

Fig. 8: The effect of corona treatment time (a) and input power (b) on the roughness parameters for the PA6/PES composite membranes.

Contact angle analysis

The contact angle tests for the untreated and corona treated membranes were also measured to determine the changes in the membrane hydrophilicity and polarity, and the results are given in Table 3. According to Table 3, the contact angle of the untreated membrane decreases from 61.3° to 15.3° for the corona treated membrane and an increase in the corona treatment time or applied power results in lower water contact angle. These results reveal that the membrane hydrophilicity increases with the membrane modification by the corona air plasma.

Gas transport properties

The gas separation performance of the dual-layer PA6/PES composite membranes before and after corona treatment was evaluated by the permeation test of O_2, N_2 and CO_2 gases and the effects of the corona applied power and exposure time on the membrane performance were investigated. The permeation properties of the untreated and corona modified membranes are given in Table 4. It can be seen that the permeability and selectivity of the untreated PA6/PES composite membrane is low. Generally, the permeability of a membrane with respect to various gases is a function of membrane physical and chemical properties, the nature of the permeant species like size, shape and polarity as well as the interaction between membrane and permeant species. The membrane properties and the nature of the permeant species determine the diffusional characteristic of a particular gas through a given membrane. The interaction between the membrane and permeant refer to the sorption of the gases in the membrane. Therefore, the sorption and diffusion of N_2, O_2 and CO_2 in the prepared dual-layer PA6/PES composite membrane is low and leads to weak gas separation properties for the selected gases. According to Table 4, the corona modification significantly affects the gas separation performance of the fabricated composite membranes.

Table 3: The water contact angle of the prepared membranes.

Membrane sample	Contact angle (°)
M1	61.3
M2	34.9
M4	28.9
M5	22.5
M6	18.5
M9	15.3

Table 4: The permeation properties of the untreated and treated PA6/PES membranes.

Membrane sample	P_{N2} (Barrer)	P_{O2} (Barrer)	P_{CO2} (Barrer)	$\alpha_{O2/N2}$	$\alpha_{CO2/N2}$
M1	1.22	1.25	0.98	1.02	0.80
M2	2.87	2.30	1.95	0.80	0.68
M3	1.70	2.71	2.19	1.59	1.29
M4	2.09	4.02	3.02	1.92	1.44
M5	0.74	3.60	9.11	4.86	12.31
M6	13.03	10.78	11.87	0.83	0.91
M7	31.24	29.81	25.64	0.95	0.82
M8	52.78	48.21	44.19	0.91	0.84
M9	76.82	72.34	66.67	0.94	0.87

Similar observations were reported in previous studies. For example, the low frequency O_2 plasma modification of polysulfone membranes[10] as well as the N_2 and NH_3 plasma treatment of different glassy and rubbery membranes improve

the gas separation performance. Two phenomena are impressive for the gas transport properties of the membrane during corona air plasma treatment. One of them is the chemical effect that introduces polar functional groups on the membrane surface. The interaction between these functional groups and permeant causes an increase in the affinity between the membrane surface and permeant and enhances the solubility of gases like CO_2 and O_2 over N_2. Another phenomenon is a physical effect that is the competitive effect between ablation of the membrane surface due to etching and deposition of etching materials and polymer fragments on the surface. These two phenomena can affect the gas separation performance of the corona modified membranes depending on the power and time of the corona treatment. The effect of corona power and exposure time on the gas permeability and selectivity are shown in Fig. 9 and 10, respectively. As indicated in Fig. 9a, when corona applied power from is varied from 240 to 400 W, the CO_2 and O_2 permeabilities increase, while the N_2 permeability slightly decreases. This behavior can be attributed to introducing functional polar groups on the membrane surface and increasing the interaction between the O_2 and CO_2 gas molecules with the membrane surface that leads to improving the sorption of the O_2 and CO_2 gas molecules into the membrane. An increase in the CO_2 and O_2 permeabilities leads to an enhancement in the CO_2/N_2 and O_2/N_2 selectivities up to 12.31 and 4.86, respectively. As the corona input power increases from 400 to 600 W, the CO_2, O_2 and N_2 permeabilities significantly enhance, and this is followed by a decrease in CO_2/N_2 and O_2/N_2 selectivities. This drastic increase in the CO_2, O_2 and N_2 permeabilities is the consequence of the creation of pinholes and cracks on the membrane surface due to the etching effect of the corona modification. These defects are highlighted on the SEM image of the M6 and M9 membrane samples (Figs. 6d and 6f). Therefore, the corona modification of the prepared PA6/PES membranes at input powers of 500 and 600 W results in membranes with low gas separation performance.

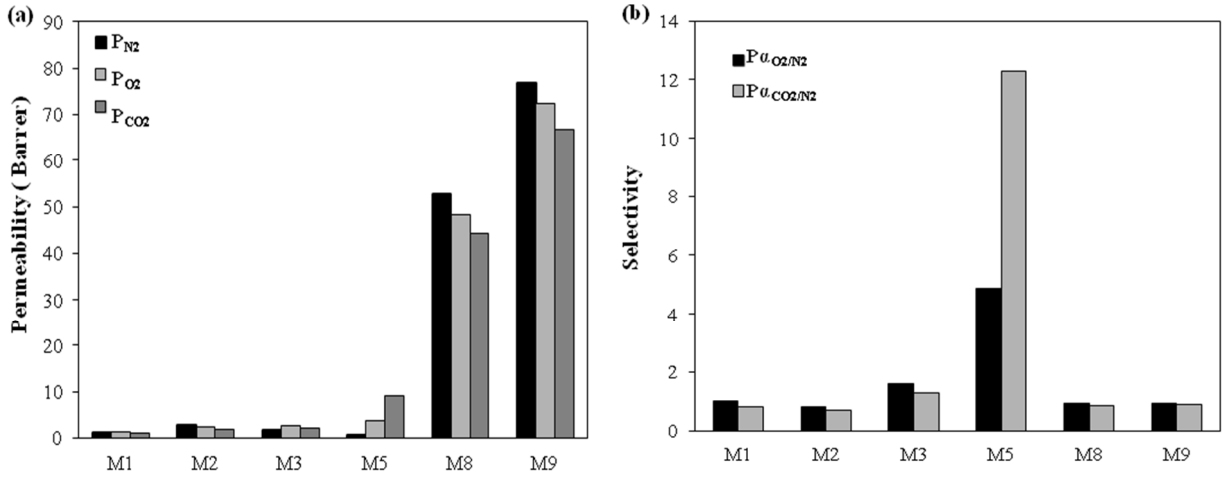

Fig. 9: The effect of corona applied power on the gas permeability (a) and selectivity (b).

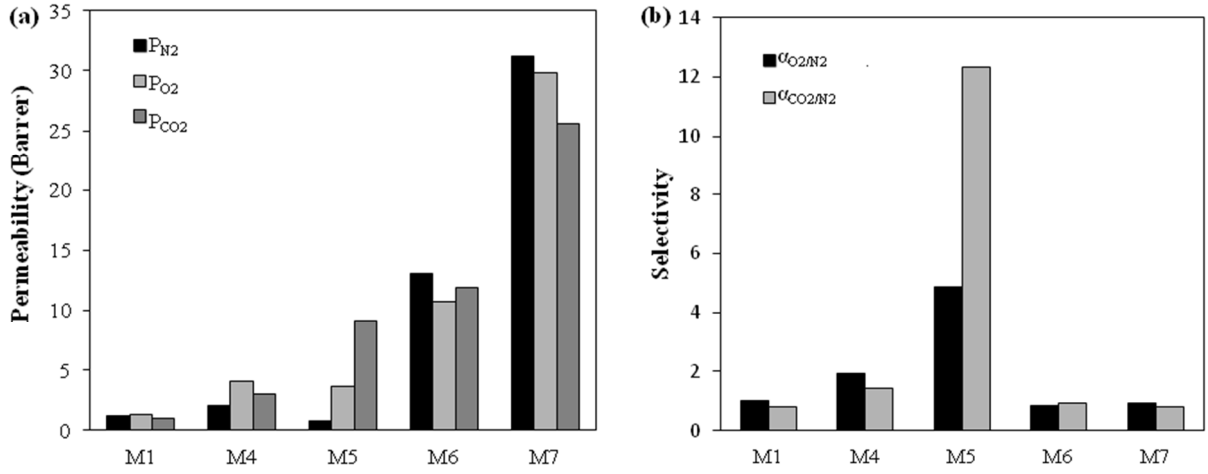

Fig. 10: The effect of corona treatment time on the gas permeability (a) and selectivity (b).

The influence of the corona treatment time on the separation performance of the membranes at corona power of 400 W is shown in Fig. 10. It can be seen that the effect of corona exposure time is similar to the influence of corona power on the gas separation performance of the membranes. When the corona exposure time varies from 2 to 4 min, the chemical effect of the corona modification is the dominant phenomenon and leads to an enhancement in the CO_2 and O_2 permeabilities as well as CO_2/N_2 and O_2/N_2 selectivities. For longer exposure times (6 and 8 min), the physical effect of the corona is the dominant phenomenon and results in modified membranes with high gas permeability and low selectivity.

Finally, for comparison purposes, the gas separation performance of different membranes reported by other research groups for N_2, O_2 and CO_2 are listed in Table 5. It can be seen that the CO_2/N_2 and O_2/N_2 selectivities of the corona modified polyamide membranes prepared in the present study are higher than those of most polyamide membranes reported in the literature.

Table 5: The gas permeability and selectivities of the modified polyamide membrane and their comparison with other gas separation membranes and some polyamides reported earlier.

Membrane	Operating Temperature (°C)	P_{N2} (Barrer)	P_{O2} (Barrer)	P_{CO2} (Barrer)	$\alpha_{O2/N2}$	$\alpha_{CO2/N2}$	Ref.
Polyamide							
Corona treated PA/PES (M1)	25	0.74	3.6	9.11	4.8	12.3	This work
PA-before annealing*	30	1.52	6.24	16.6	4.1	10.9	29
PA-after annealing*	30	0.95	5.13	15.2	5.4	16.0	29
Polymer 1a**	-	29.00	49.62	195.37	1.7	6.7	30
Polymer 1b**	-	53.84	107.91	460.53	2.0	8.5	30
Poly(ether amide)							
PA 9A	35	1.30	9.50	34.00	7.3	26.0	31
PA 9B	35	1.00	8.20	29.00	8.2	29.0	31
PA 9C	35	0.60	3.50	13.00	5.8	21.7	31
Poly(aryl ether ketone)							
PEK-C	30	0.15	0.95	2.73	6.2	17.8	32
IMPEK-C	30	0.93	4.85	19.30	5.2	20.7	32
Poly(aryl ether sulfone)							
PES-C	30	0.17	0.95	5.74	5.6	34.4	33
IMPES-C	30	0.70	4.85	19.40	5.5	27.7	33
Cellulose acetate	30	0.21	0.59	6.30	2.8	30.0	34
Polycarbonate	30	0.18	1.36	4.23	7.6	23.5	34
Polyimide	30	0.32	2.13	10.70	6.6	33.4	34
Polydimethylsiloxane	30	250	500	800	2.0	3.2	34
		299	540	1300	1.8	4.3	35
Polyphenyleneoxide	30	3.81	16.80	75.80	4.4	19.9	34
Polysulfone	30	0.25	1.40	5.60	5.6	22.4	34
		0.80	1.70	6.10	2.1	7.6	35
Polystyrene	30	0.60	2.40	10.40	4.0	17.3	35
Polymethylmethacrylate	30	1.20	3.30	0.60	2.7	0.5	35
Polyethylene	30	4.20	6.30	17.90	1.5	4.2	35
Polyvinylacetate	30	1.30	2.30	13.10	1.8	10.1	35

* Permeance value in GPU= 7.5×10^{-12} $m^3/(m^2\ s\ Pa)$

** Permeance value in 10^{-3} $m^3/(m^2\ h\ bar)$

Conclusions

Dual-layer polyamide 6/polyethersulfone composite membranes were fabricated via the phase inversion techniques for the gas separation applications and the corona air plasma was successfully used to modify the surface of the prepared membranes in order to improve the separation performance. The effect of corona treatment time and input power on the surface properties and separation performance of the membranes was studied. The FTIR-ATR analysis of the untreated and corona treated PA6/PES membranes showed the composition and absorbance intensity of some functional groups such as C=O, C-N and amides groups on the membrane surface altered by the corona air plasma treatment. Existence of these polar groups on the surface increases the polarity of the membrane and chemical affinity between CO_2 and O_2 and the membrane surface. The maximum intensity of these favorable functional groups was detected for corona treatment conditions of 400W and 4 min. The SEM and AFM analysis indicated that when the membrane was treated by corona at different treatment times and powers, different phenomena including etching which led to surface roughening, formation of polar bonds and deposition of etching materials occurred. However, prolonged corona treatment caused formation of cracks and defects on the membrane surface. The gas separation properties of the modified membrane were changed considerably with the corona treatment time and power and the maximum selectivity of CO_2/N_2 and O_2/N_2 was observed for the treatment condition of 400 W and 4 min.

Finally, it can be concluded that the corona air plasma is a useful technique for the membrane modification that changes the surface properties of the PA6/PES membranes and leads to

improvement of the gas separation properties of the membrane without damaging the selective layer of the membrane at optimum treatment conditions.

References

1. R. W. Baker, *Industrial & Engineering Chemistry Research*, 2002, **41**, 1393.
2. C. A. Scholes, G. W. Stevens and S. E. Kentish, *Fuel*, 2012, **96**, 15.
3. S. D. Kenarsari, D. Yang, G. Jiang, S. Zhang, J. Wang, A. G. Russell, Q. Wei and M. Fan, *RSC Advances*, 2013, **3**, 22739.
4. D. Bastani, N. Esmaeili and M. Asadollahi, *Journal of Industrial and Engineering Chemistry*, 2013, **19**, 375.
5. D. F. Sanders, Z. P. Smith, R. Guo, L. M. Robeson, J. E. McGrath, D. R. Paul and B. D. Freeman, *Polymer*, 2013, **54**, 4729.
6. D. Bera, P. Bandyopadhyay, S. Ghosh and S. Banerjee, *Journal of Membrane Science*, 2014, **453**, 175.
7. K. Fatyeyeva, A. Dahi, C. Chappey, D. Langevin, J.-M. Valleton, F. Poncin-Epaillard and S. Marais, *RSC Advances*, 2014, **4**, 31036.
8. P. Attri, B. Arora and E. H. Choi, *RSC Advances*, 2013, **3**, 12540.
9. A. Lin, S. Shao, H. Li, D. Yang and Y. Kong, *Journal of Membrane Science*, 2011, **371**, 286.
10. X. Wei, B. Zhao, X.-M. Li, Z. Wang, B.-Q. He, T. He and B. Jiang, *Journal of Membrane Science*, 2012, **407–408**, 164.
11. M. L. Steen, L. Hymas, E. D. Havey, N. E. Capps, D. G. Castner and E. R. Fisher, *Journal of Membrane Science*, 2001, **188**, 97.
12. B. Jaleh, P. Parvin, P. Wanichapichart, A. P. Saffar and A. Reyhani, *Applied Surface Science*, 2010, **257**, 1655.
13. D. Tyszler, R. G. Zytner, A. Batsch, A. Brügger, S. Geissler, H. Zhou, D. Klee and T. Melin, *Desalination*, 2006, **189**, 119.
14. I. Sadeghi, A. Aroujalian, A. Raisi, B. Dabir and M. Fathizadeh, *Journal of Membrane Science*, 2013, **430**, 24.
15. N. Hilal, M. Khayet ,C.J. Wright, *Membrane Modification: Technology and Applications*, CRC Press, United State of America, 2012.
16. D. E. Weibel, C. Vilani, A. C. Habert and C. A. Achete, *Surface and Coatings Technology*, 2006, **201**, 4190.
17. L.P. Zhu, B.K. Zhu, L. Xu, Y.X. Feng, F. Liu and Y.Y. Xu, *Applied Surface Science*, 2007, **253**, 6052.
18. H. Guo, C. Geng, Z. qin and C. Chen, *Desalination and Water Treatment*, 2013, **51**, 3810.
19. K. S. Kim, K. H. Lee, K. Cho and C. E. Park, *Journal of Membrane Science*, 2002, **199**, 135.
20. M. Bryjak, I. Gancarz, G. Poźniak and W. Tylus, *European Polymer Journal*, 2002, **38**, 717.
21. V. Moghimifar, A. Raisi and A. Aroujalian, *Journal of Membrane Science*, 2014, **461**, 69.
22. M. Nakata and H. Kumazawa, *Journal of Applied Polymer Science*, 2006, **101**, 383.
23. T. Teramae and H. Kumazawa, *Journal of Applied Polymer Science*, 2007, **104**, 3236.
24. H. Kumazawa and M. Yoshida, *Journal of Applied Polymer Science*, 2000, **78**, 1845.
25. R. K. Y. Fu, I. T. L. Cheung, Y. F. Mei, C. H. Shek, G. G. Siu, P. K. Chu, W. M. Yang, Y. X. Leng, Y. X. Huang, X. B. Tian and S. Q. Yang, *Nuclear Instruments and Methods in Physics Research Section B: Beam Interactions with Materials and Atoms*, 2005, **237**, 417.
26. S. Modarresi, M. Soltanieh, S. A. Mousavi and I. Shabani, *Journal of Applied Polymer Science*, 2012, **124**, E199-E204.
27. E. F. Castro Vidaurre, C. A. Achete, F. Gallo, D. Garcia, R. Simao and A. C. Habert, *Materials Research*, 2002, **5**, 37.
28. K. K. Samanta, M. Jassal and A. K. Agrawal, *Surface and Coatings Technology*, 2009, **203**, 1336.
29. S. Sridhar, B. Smitha, S. Mayor, B. Prathab and T. M. Aminabhavi, Journal of Materials Science, 2007, **42**, 9392-9401.
30. J. Petersen and K.V. Peinemann, Journal of Applied Polymer Science, 1997, **63**, 1557-1563.
31. D. Bera, P. Bandyopadhyay, S. Ghosh and S. Banerjee, Journal of Membrane Science, 2014, **453**, 175-191.
32. Z. Wang, T. Chen and J. Xu, Macromolecules, 2000, **33**, 5672-5679.
33. Z. Wang, T. Chen and J. Xu, Macromolecules, 2001, **34**, 9015-9022.
34. V. Abetz, T. Brinkmann, M. Dijkstra, K. Ebert, D. Fritsch, K. Ohlrogge, D. Paul, K.-V. Peinemann, S.P. Nunes, N. Scharnagk and M. Schossig, Advanced Engineering Materials, 2006, **8**, 328-358.
35. C.J. Orme, M.L. Stone, M.T. Benson and E.S. Peterson, Separation Science Technology, 2003, **38**, 3225-3238.